nature immunology

A sestrin-dependent Erk–Jnk–p38 MAPK activation complex inhibits immunity during aging

Alessio Lanna[1,2], Daniel C O Gomes[1,3], Bojana Muller-Durovic[1], Thomas McDonnell[1], David Escors[1,4], Derek W Gilroy[5], Jun Hee Lee[6], Michael Karin[7] & Arne N Akbar[1]

Mitogen-activated protein kinases (MAPKs) including Erk, Jnk and p38 regulate diverse cellular functions and are thought to be controlled by independent upstream activation cascades. Here we show that the sestrins bind to and coordinate simultaneous Erk, Jnk and p38 MAPK activation in T lymphocytes within a new immune-inhibitory complex (sestrin–MAPK activation complex (sMAC)). Whereas sestrin ablation resulted in broad reconstitution of immune function in stressed T cells, inhibition of individual MAPKs allowed only partial functional recovery. T cells from old humans (>65 years old) or mice (16–20 months old) were more likely to form the sMAC, and disruption of this complex restored antigen-specific functional responses in these cells. Correspondingly, sestrin deficiency or simultaneous inhibition of all three MAPKs enhanced vaccine responsiveness in old mice. Thus, disruption of sMAC provides a foundation for rejuvenating immunity during aging.

Aging is associated with a substantial decline in immune function that manifests as increased incidence of infection and malignancy and decreased responsiveness to vaccination[1,2]. Given the worldwide demographic shift toward older populations[3], it is essential to understand mechanisms involved with age-related decline of immunity and identify strategies for restoring immune function. Published studies suggest causative links between immunosenescence, metabolism and aging and reveal that the age-associated decline in immune function may be partially reversible[4–8]. However, how the myriad of functional defects simultaneously appear in individual aged cells remains largely unknown.

Human T cells showing multiple features of senescence increase in number during aging[9]. There is a sequential loss of the costimulatory receptors CD27 and CD28 as T cells progress toward senescence[10]. Early-stage T cells within the CD4 compartment are $CD27^+CD28^+$, those at an intermediate stage are $CD27^-CD28^+$, and senescent T cells are $CD27^-CD28^-$ (ref. 5).

MAPKs are signal-transducing enzymes involved in diverse aspects of mammalian physiology, including senescence, aging and metabolism[11]. Three main subgroups of MAPKs have been identified: Erk, Jnk and p38 (ref. 12). Given the broad functions they control and the existence of independent upstream activation cascades, it is thought that each MAPK subgroup is separately regulated within individual cells[12–14]. The possibility that all three MAPK subgroups may be coordinately controlled within a single cell type has remained unexplored.

Sestrins, the mammalian products of the *Sesn1*, *Sesn2* and *Sesn3* genes[15–17], are poorly understood stress-sensing proteins that lack obvious catalytic domains and stimulate the activation of AMPK by an unknown mechanism while inhibiting mammalian target of rapamycin complex 1 (mTORC1) signaling[18]. AMPK is a heterotrimeric protein consisting of the catalytic α-subunit and the regulatory β- and γ-subunits that are activated in response to increased intracellular AMP/ATP ratio[19]. Sestrins have been proposed to inhibit mTORC1 signaling through both AMPK-dependent and independent pathways that involve formation of a complex with the Rag GTPases[18,20–25]. Owing to their mTORC1 inhibitory activity, various anti-aging functions have been ascribed to both the mammalian sestrins and their *Drosophila* counterpart, dSesn[20]. However, whether sestrins have a role in the control of the immune response has not been determined.

In this study, we found that sestrins have pro-aging activities in T lymphocytes. We identified a sestrin-dependent MAPK activation complex (termed sMAC), in which sestrins simultaneously coordinate the activation of Erk, Jnk and p38 in these cells. We found that each MAPK, once activated, controls a unique functional response. Disruption of the sMAC restored antigen-specific proliferation and cytokine production in T cells from old humans and enhanced responsiveness to influenza vaccination in old mice.

RESULTS

Sestrins are broad regulators of T cell senescence

The sestrins have anti-aging properties in muscle[20], but their functions in the immune system have not been studied. We examined

[1]Division of Infection and Immunity, University College London, London, UK. [2]Nuffield Department of Medicine, University of Oxford, Oxford, UK. [3]Núcleo de Doenças Infecciosas/Núcleo de Biotecnologia, Universidade Federal do Espírito Santo - UFES, Vitória, Brazil. [4]Navarrabiomed-Biomedical Research Centre, Fundación Miguel Servet, IdisNA, Complejo Hospitalario de Navarra, Pamplona, Spain. [5]Division of Medicine, University College London, London, London, UK. [6]Department of Molecular and Integrative Physiology, University of Michigan, Ann Arbor, Michigan, USA. [7]Laboratory of Gene Regulation and Signal Transduction, Departments of Pharmacology and Pathology, University of California, San Diego School of Medicine, La Jolla, California, USA. Correspondence should be addressed to A.N.A. (a.akbar@ucl.ac.uk) or A.L. (alessio.lanna@kennedy.ox.ac.uk).

Received 27 July 2016; accepted 15 December 2016; published online 23 January 2017; doi:10.1038/ni.3665

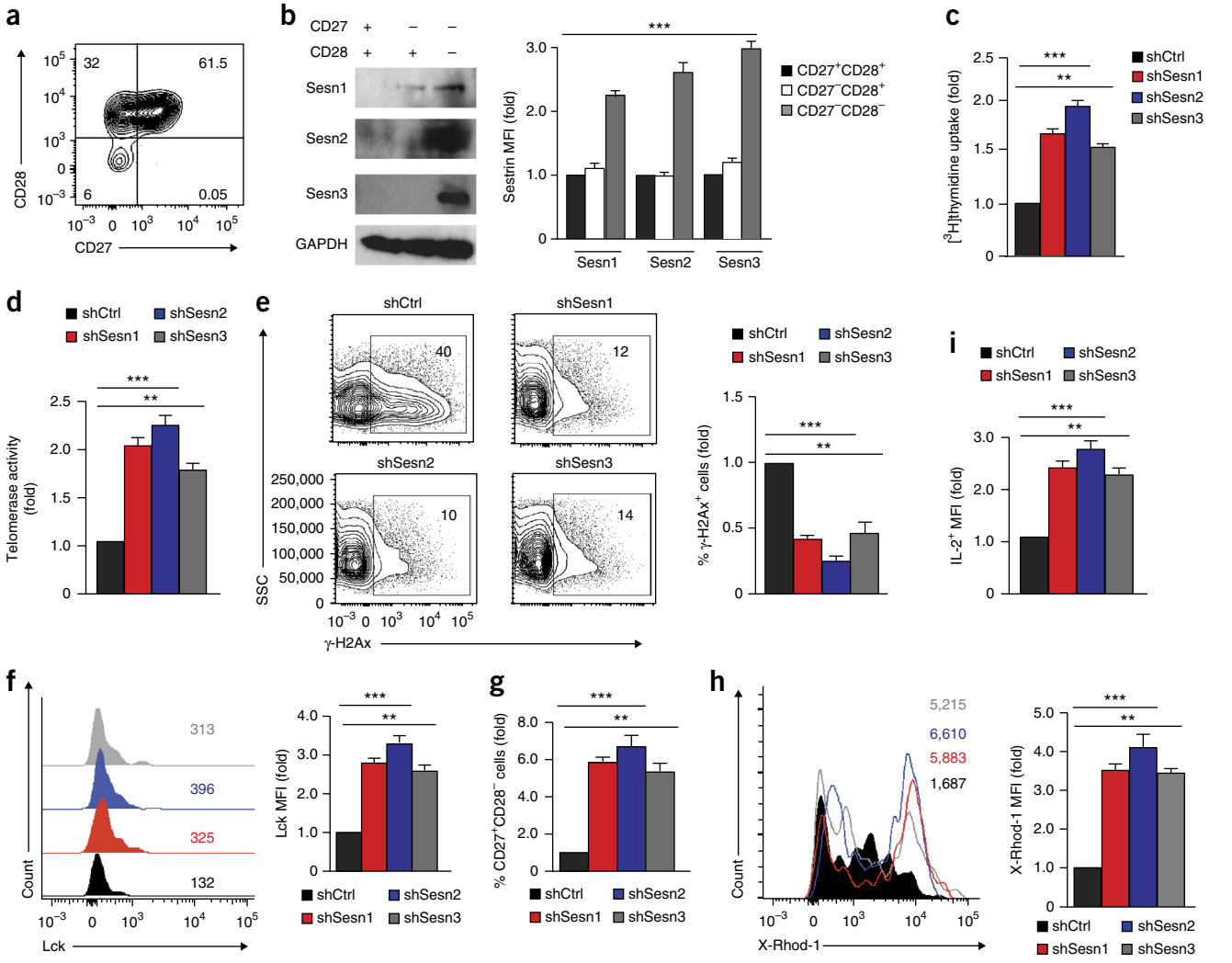

Figure 1 Sestrins are broad regulators of T cell senescence. (**a**) Expression of surface CD27 and CD28 in human CD4+ T cells by flow cytometry. Numbers in quadrants indicate cell percentages. (**b**) Immunoblot analysis (left) and mean fluorescence intensity (MFI) data (right) of endogenous sestrin 1 (Sesn1), sestrin 2 (Sesn2) and sestrin 3 (Sesn3) expression in CD4+ T cells gated as in **a**. Data are presented relative to results in $CD27^+CD28^+$ cells. (**c**,**d**) Cell proliferation as assessed by [3H]thymidine uptake (**c**) and telomerase activity (**d**) in $CD27^-CD28^-CD4^+$ T cells transduced with various shRNAs. (**e**) DNA damage foci assessed by the DNA damage response marker γ-H2Ax in cells as above. (**f**–**i**) Flow cytometry analysis of intracellular Lck (**f**), CD27 and CD28 costimulatory receptor expression (**g**), calcium abundance (assessed by X-Rhod-1 fluorescence) (**h**) and IL-2 synthesis (**i**) in $CD27^-CD28^-CD4^+$ T cells transduced with various shRNAs. Numbers in quadrants, MFI. Results are presented relative to those of cells transduced with shCtrl, set as 1. Data are representative of 4 experiments (**a** and **b**, left) or pooled from 4 experiments with 4 individual donors (**b**, right) or 3 donors (**c**–**i**). $^{**}P < 0.01$, $^{***}P < 0.001$ ANOVA for repeated measures with Bonferroni post-test correction. Error bars indicate s.e.m. Uncropped blots are shown in **Supplementary Figure 8**.

the expression of sestrin 1, sestrin 2 and sestrin 3 proteins in blood-derived primary human CD4+ T cells from young donors (<40 years old) defined as nonsenescent ($CD27^+CD28^+$), intermediate ($CD27^-CD28^+$) or senescent ($CD27^-CD28^-$) CD4+ T cells as described[5]. $CD27^-CD28^-CD4^+$ T cells expressed significantly higher amounts of sestrin 1, sestrin 2 and sestrin 3 than $CD27^+CD28^+CD4^+$ or $CD27^-CD28^+CD4^+$ T cells (**Fig. 1a**,**b**). We probed the function of endogenous sestrin proteins by transducing activated $CD27^-CD28^-CD4^+$ T cells with lentiviral vectors coexpressing a GFP reporter and inhibitory small hairpin RNAs (shRNAs) targeting *SESN1* (shSesn1), *SESN2* (shSesn2) or *SESN3* (shSesn3). A nonsilencing shRNA lentiviral vector was used as a control (shCtrl) (**Supplementary Fig. 1a**–**c**). Compared to shCtrl-transduced controls, $CD27^-CD28^-$ T cells transduced with shSesn1, shSesn2 or shSesn3 showed broad functional reversal of senescence, apparent as enhancement of cell proliferation (**Fig. 1c**) and telomerase activity (**Fig. 1d**), fewer DNA damage foci (**Fig. 1e**) and re-expression of the TCR signalosome components Lck and Zap70 (**Fig. 1f** and data not shown) and the costimulatory receptors CD27 and CD28 (**Fig. 1g**). This enhancement of functionality in $CD27^-CD28^-CD4^+$ T cells was accompanied by restored calcium flux (**Fig. 1h**) and IL-2 synthesis (**Fig. 1i**). Therefore, in contrast to their well-documented anti-aging properties in invertebrates[20,26], the sestrins induced multiple characteristics of senescence in T cells.

Sestrins bind and activate MAPKs in $CD27^-CD28^-CD4^+$ T cells

In *Drosophila*, mouse liver homogenates and human embryonic kidney (HEK293) cells, sestrin function, including the anti-aging

effects, is largely mTORC1 dependent[20,21,23–25,27,28]. We found that CD27$^-$CD28$^-$CD4$^+$ T cells lacked expression of both the kinase mTOR and its downstream effector kinase S6K1 (**Supplementary Fig. 1d**). Transduction of shSesn1, shSesn2 or shSesn3 in CD27$^-$CD28$^-$CD4$^+$ T cells restored both mTOR expression and downstream S6K1 activation (**Supplementary Fig. 1e**). However, these cells maintained significantly ($P < 0.01$, ANOVA for repeated measures with a Bonferroni post-test correction) higher calcium flux (**Supplementary Fig. 1f**), interleukin 2 (IL-2) synthesis (**Supplementary Fig. 1g**), telomerase activity (**Supplementary Fig. 1h**) and clearance of DNA damage foci (**Supplementary Fig. 1i**) than that of shCtrl-transduced cells, even in the presence of the mTOR inhibitor rapamycin. This indicates an mTORC1-independent mechanism of sestrin action.

To identify pro-senescence pathways of sestrin action, we immunoprecipitated sestrin 1 from blood-derived, unstimulated CD27$^-$CD28$^-$CD4$^+$ T cells using an irrelevant IgG antibody as a control. Compared to IgG immunoprecipitates, sestrin 1 immunoprecipitates were enriched for phosphorylated Erk, Jnk and p38 MAPKs[12] (**Fig. 2a**). Phosphorylated AMPK also precipitated with sestrin 1 (**Fig. 2a**). Similarly, sestrin 2 coimmunoprecipitated with phosphorylated Erk, Jnk and p38 in CD27$^-$CD28$^-$CD4$^+$ T cells (**Supplementary Fig. 2a**). This suggests the presence of an endogenous supramolecular sMAC composed of sestrins and phosphorylated AMPK and Erk and Jnk and p38 MAPKs.

Next we measured spontaneous Erk, Jnk and p38 MAPK activation in blood-derived CD27$^+$CD28$^+$, CD27$^-$CD28$^+$ and CD27$^-$CD28$^-$ T cells within the CD4$^+$ subset. Endogenous MAPK activation was enhanced in CD27$^-$CD28$^-$ T cells compared to CD27$^+$CD28$^+$ or CD27$^-$CD28$^+$ T cell subsets (**Supplementary Fig. 2b**). To investigate canonical MAPK activators, we probed lysates from CD27$^+$CD28$^+$, CD27$^-$CD28$^+$ and CD27$^-$CD28$^-$CD4$^+$ T cell subsets directly *ex vivo* with antibodies to MKK7 (activator of Jnk), MKK4 (activator of Jnk and/or p38) and phosphorylated MEKK1 and MEKK2 (activators of Erk). CD27$^-$CD28$^-$ T cells did not express or endogenously activate any upstream MKK4, MKK7 or MEKK1 and MEKK2 molecules (**Supplementary Fig. 2c**). We next transfected small interfering RNAs (siRNAs) targeting MEKK1, MKK7 and MKK4 in CD27$^+$CD28$^+$CD4$^+$ and CD27$^-$CD28$^-$CD4$^+$ T cell subsets and measured Erk, Jnk and p38 phosphorylation in both cell types by phospho-flow technology. A scrambled siRNA was used as control (**Supplementary Fig. 2d**). Compared to control transfection, siRNAs against MEKK1, MKK7 and MKK4 inhibited Erk, Jnk and p38 phosphorylation in CD27$^+$CD28$^+$CD4$^+$ T cells, respectively. In contrast, Erk, Jnk and p38 phosphorylation were not affected in CD27$^-$CD28$^-$CD4$^+$ T cells (**Supplementary Fig. 2e**). Thus, endogenous MAPK phosphorylation in CD27$^-$CD28$^-$ T cells takes place in the absence of upstream canonical MAPK signaling[11].

We next investigated whether sestrins are noncanonical regulators of MAPK function. *In vitro* kinase assays demonstrated disrupted MAPK phosphorylation in AMPK immunoprecipitates from CD27$^-$CD28$^-$CD4$^+$ T cells transduced with shRNAs against sestrins 1–3 (triple-knockdown cells) compared to those transduced with shCtrl (**Fig. 2b**). However, treatment of triple-knockdown T cells with the selective AMPK agonist A-769662 (ref. 29) for 1 h reconstituted MAPK activation to levels detected with shCtrl transduction (**Fig. 2b**). We then transduced shAMPK[5] and shCtrl vectors in CD27$^-$CD28$^-$CD4$^+$ T cells, immunoprecipitated sestrin 2 and performed *in vitro* MAPK assays. MAPK phosphorylation was reduced in sestrin 2 immunoprecipitates from shAMPK-transduced CD27$^-$CD28$^-$CD4$^+$ T cells compared to shCtrl-transduced cells (**Supplementary Fig. 2f**). Thus, sestrins promote MAPK activation via AMPK.

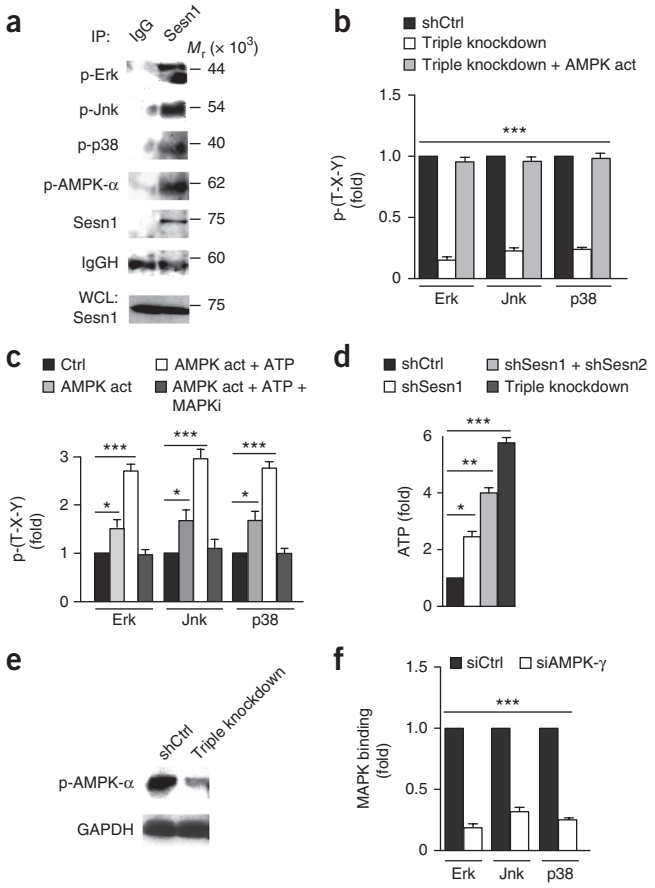

Figure 2 Sestrins bind to and activate Erk, Jnk and p38 in CD27$^-$CD28$^-$CD4$^+$ T cells. (**a**) Immunoblot analysis of lysates from CD27$^-$CD28$^-$CD4$^+$ T cells precipitated with IgG control or anti–sestrin 1 (Sesn1) and stained for Sesn1 and phosphorylated (p-) MAPKs. IP, immunoprecipitation; WCL, whole cell lysates. (**b**) MAPK phosphorylation, indicated by phosphorylation of the Thr-Xaa-Tyr loop (p-(T-X-Y)), of AMPK-α immunoprecipitates from shCtrl-transduced or triple-knockdown CD27$^-$CD28$^-$CD4$^+$ T cells treated or not with the AMPK agonist A-769662 (AMPK act; 150 μM, 60 min) 96 h later. Results are presented relative to shCtrl, set as 1. (**c**) MAPK autophosphorylation in sestrin 1 complexes from CD27$^-$CD28$^-$CD4$^+$ T cells incubated for 30 min with or without (Ctrl) A-769662 (150 μM) and MAPKi FR18024 (20 μM; Erk), SP-600125 (10 μM; Jnk) or SB-203580 (10 μM; p38) in the presence or absence of ATP (200 μM). MAPK activity was determined and presented as in **b**. (**d**) ELISA-based ATP abundance in AMPK-γ immunoprecipitates from CD27$^-$CD28$^-$CD4$^+$ T cells wherein one or more sestrins were silenced by shRNA. Results are presented relative to that of cells transduced with shCtrl, set as 1. (**e**) AMPK phosphorylation of cells as in **d**; GAPDH, loading control. (**f**) ELISA-based MAPK binding assays in sestrin 1 immunoprecipitates from cells as in **a** transfected with siCtrl or siAMPK-γ for 36 h. Results are presented relative to those of cells transfected with siCtrl, set as 1. Data are representative of 2 (**a**) or 3 (**e**) experiments or pooled from 3 independent experiments with 3 individual donors (**b**–**d**, **f**). $^*P < 0.05$, $^{**}P < 0.01$, $^{***}P < 0.001$, ANOVA for repeated measures with Bonferroni post-test correction. Error bars indicate s.e.m. Uncropped blots are shown in **Supplementary Figure 8**.

Because the dual phosphorylation site of MAPK proteins (a Thr-Xaa-Tyr motif within the activation loop) is not a direct AMPK substrate[5], we investigated whether sestrin-bound MAPKs undergo AMPK-dependent autophosphorylation. Adding exogenous ATP to sestrin 1 immunoprecipitates from CD27$^-$CD28$^-$CD4$^+$ T cells

strongly enhanced MAPK phosphorylation in response to incubation with A-769662 compared to unstimulated reactions (**Fig. 2c**). The ATP-competitive Erk inhibitor FR18024, the Jnk inhibitor SP-600125 and the p38 inhibitor SB-203580 each impeded AMPK agonist–driven MAPK phosphorylation (**Fig. 2c**). Thus, individual MAPK activities are required for sMAC activation. Furthermore, MAPK autophosphorylation is triggered by activation of AMPK.

We next tested whether sestrins modulate MAPK signaling by promoting ATP removal from the γ subunit of AMPK[28]. We therefore transduced $CD27^-CD28^-CD4^+$ T cells with the sestrin-specific shRNAs individually and together, then immunoprecipitated AMPK-γ and measured ATP content by ELISA. The ATP contents in AMPK-γ immunoprecipitates from $CD27^-CD28^-CD4^+$ T cells increased alongside progressive single, dual or triple silencing of sestrin proteins (**Fig. 2d**). Similarly, phosphorylation of AMPK-α, the catalytic subunit of the enzyme, was inhibited in extracts from triple-knockdown $CD27^-CD28^-CD4^+$ T cells compared to shCtrl transduction (**Fig. 2e**). In addition, when we transfected $CD27^-CD28^-CD4^+$ T cells with siRNA targeting AMPK-γ (**Supplementary Fig. 2f**) and immunoprecipitated sestrin 1, we found lower Erk, Jnk and p38 MAPK expression in the sestrin 1 complex, as compared to cells transfected with control siRNA (siCtrl) (**Fig. 2f**). Thus, sestrins regulate Erk, Jnk and p38 MAPK autophosphorylation by fine-tuning AMPK-γ ATP loading.

Recombinant sestrins reconstitute sMAC

We performed *in vitro* reconstitution experiments using lysates from $CD27^+CD28^+CD4^+$ T cells, which do not express endogenous sestrin proteins. We transfected siAMPK-γ or siCtrl into $CD27^+CD28^+$ T cells that were lysed and immunoprecipitated with antibodies to AMPK-α 36 h later. We then added either recombinant sestrins 1, 2 and/or 3 or GFP proteins and measured Erk, Jnk and p38 phosphorylation. The addition of sestrins triggered dose-dependent activation of AMPK-associated MAPKs in lysates from siCtrl-transfected $CD27^+CD28^+CD4^+$ T cells compared to recombinant GFP protein (**Fig. 3a**). In contrast, siAMPK-γ transfection in $CD27^+CD28^+CD4^+$ T cells prevented sestrin-driven MAPK activation (**Fig. 3a**). MAPK recruitment to AMPK was not significantly altered by recombinant sestrins in these *in vitro* reconstitution assays (**Fig. 3b**). These data suggest that sestrins coordinate the sMAC upstream of AMPK-γ and that all MAPKs are bound to AMPK in their inactive form.

To study whether the sMAC formed as a unique complex, we added sestrins 1–3 to lysates of blood-derived primary human $CD27^+CD28^+CD4^+$ T cells then analyzed sestrin 2 immunoprecipitates using gel-filtration chromatography. Under native conditions, the sMAC eluted with an estimated molecular mass of ~1,000 kDa (**Fig. 3c**), whereas the sestrin–mTORC1 inhibitory complex, which contains GATOR2 and RagA and RagB[23–25], was 660 kDa (**Fig. 3c**). Endogenous complexes of similar size were eluted from lysates obtained from $CD27^+CD28^+CD4^+$ T cells that had been glucose starved for 12 h (ref. 5) and immunoprecipitated with sestrin 2 (data not shown), indicating that physiological stress stimuli also triggered the formation of two sestrin-containing complexes of different sizes, controlling either mTORC1 or MAPK activities in primary human $CD27^+CD28^+CD4^+$ T cells.

To determine the physiological impact of endogenous sMAC formation in $CD27^+CD28^+CD4^+$ T cells, we transduced these cells either with shSesn1, shSesn2 and shSesn3 or with shCtrl lentiviral vectors and exposed them to irradiation to induce a stress response. Sestrin expression was upregulated in $CD27^+CD28^+$ T cells after irradiation (**Supplementary Fig. 3a**). Notably, phosphorylation of Erk, Jnk and p38 was strongly induced upon irradiation of shCtrl-transduced $CD27^+CD28^+CD4^+$ T cells compared to triple-knockdown $CD27^+CD28^+CD4^+$ T cells (**Fig. 3d**). Notably, triple knockdown of sestrin in irradiated $CD27^+CD28^+CD4^+$ T cells preserved telomerase activity (**Supplementary Fig. 3b**) and IL-2 production (**Supplementary Fig. 3c**). Sestrin-knockdown $CD27^+CD28^+$ T cells also showed lower irradiation-triggered DNA damage (**Supplementary Fig. 3d**), indicating that sestrin expression is required for induction of senescence in stressed T cells.

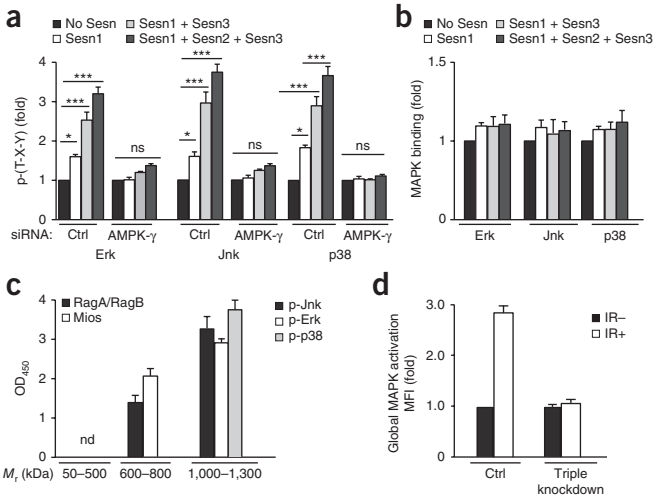

Figure 3 Reconstitution of the sMAC in $CD27^+CD28^+CD4^+$ T cells. (**a**) ELISA-based MAPK phosphorylation in AMPK-α immunoprecipitates from $CD27^+CD28^+CD4^+$ T cells transfected with various siRNAs, lysed 36 h later and incubated with either GFP (no Sesn) or recombinant human sestrins (Sesn1, Sesn2 and/or Sesn3, 1 μg/mL each) for 1 h. Sestrin-dependent MAPK activation is presented relative to that of GFP-treated extracts (no Sesn), set as 1. (**b**) ELISA-based MAPK binding in lysates from $CD27^+CD28^+CD4^+$ T cells after incubation with recombinant sestrins for 1 h followed by immunoprecipitation with antibodies to AMPK-α. MAPK recruitment to AMPK is presented relative to that of GFP-treated extracts (no Sesn). (**c**) Gel-filtration chromatography coupled to ELISA-binding assays of sestrin 2 complexes from $CD27^+CD28^+CD4^+$ T cells after incubation with recombinant sestrins. p-, phosphorylated. (**d**) Irradiation (IR)-triggered Erk, Jnk and p38 phosphorylation in shCtrl-transduced (Ctrl) or triple-knockdown $CD27^+CD28^+CD4^+$ T cells analyzed by phospho-flow cytometry 8 h after irradiation. Data are pooled from 3 (**a**) or 2 (**b**–**d**) independent experiments. ns, not significant, $*P < 0.05$, $**P < 0.01$, $***P < 0.001$, ANOVA for repeated measures with Bonferroni post-test correction. Error bars indicate s.e.m. MFI, mean fluorescence intensity. nd, not detected.

Each MAPK controls distinct aspects of T cell senescence

Because all three MAPKs were activated in the sMAC after AMPK activation, we investigated the role of each MAPK in this complex. We treated $CD27^-CD28^-CD4^+$ T cells with MAPK inhibitor (MAPKi) FR18024 (an Erk inhibitor), SP-600125 (a Jnk inhibitor) or SB-203580 (a p38 inhibitor) for 36 h before immunoprecipitating sestrin 1 and measuring Erk, Jnk and p38 phosphorylation. Endogenous MAPK phosphorylation of sestrin 1–associated MAPKs was inhibited in MAPKi-treated $CD27^-CD28^-CD4^+$ T cells but not in cells treated with DMSO (**Supplementary Fig. 4a**). In these experiments, blocking any MAPK increased CD3- and recombinant human IL-2 (rhIL-2)-induced proliferation of $CD27^-CD28^-CD4^+$ T cells by 2- to 2.5-fold, as compared to cells treated with DMSO vehicle (**Supplementary Fig. 4b**).

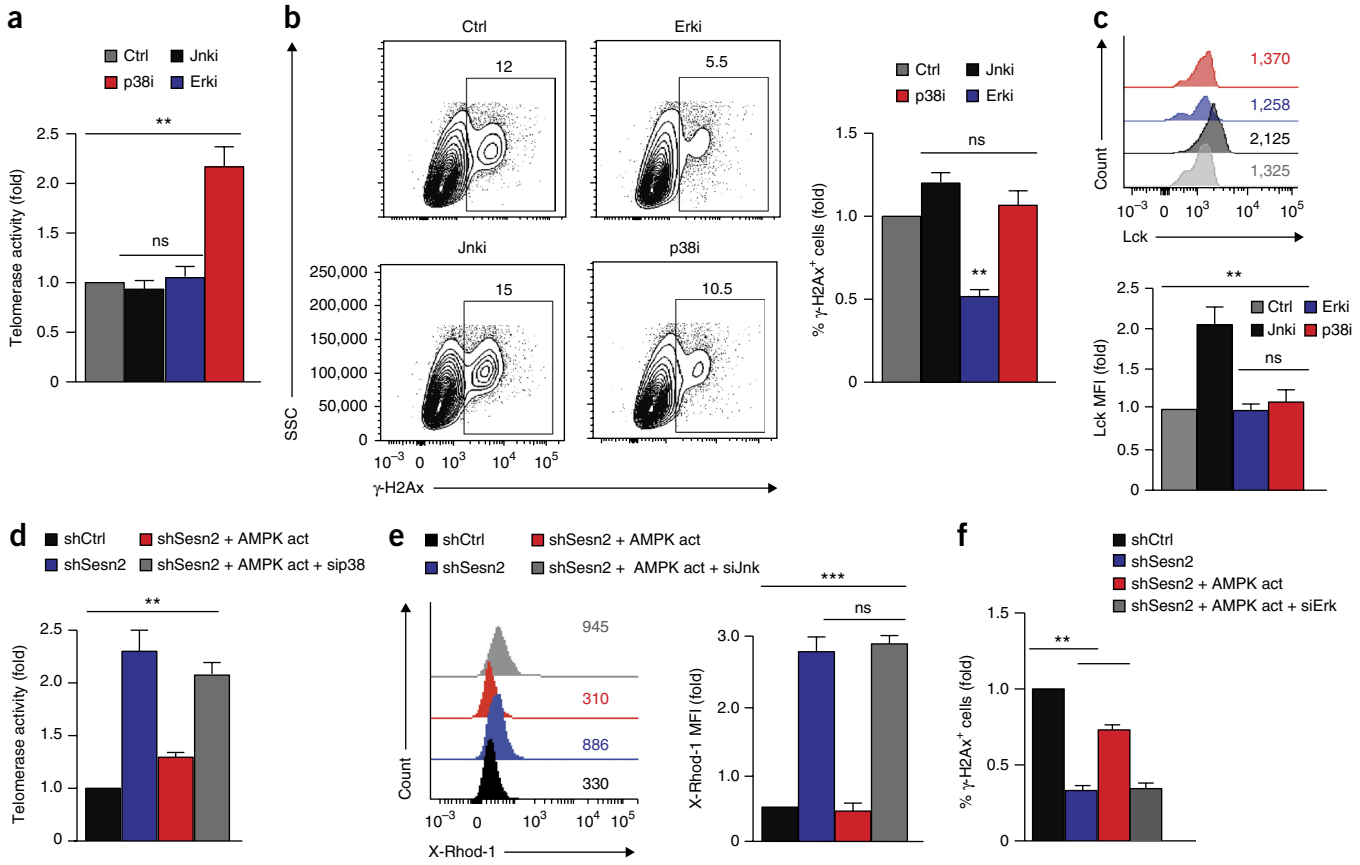

Figure 4 Individual MAPKs control different aspects of T cell senescence. (**a**–**c**) Measurement of telomerase activity (**a**), endogenous DNA damage response (DDR) foci (**b**) and expression of the TCR signalosome component Lck (**c**) in CD27$^-$CD28$^-$CD4$^+$ T cells treated with the Erk inhibitor FR18024 (Erki, 20 μM), the Jnk inhibitor SP-600125 (Jnki, 10 μM) or the p38 inhibitor SB-203580 (p38i, 10 μM) for 36 h then analyzed for functional readouts. A DMSO solution was used as control (ctrl). (**d**–**f**) Effect of siRNAs on telomerase activity (**d**), calcium flux (**e**) and DDR γ-H2Ax foci (**f**) in shSesn2-transduced CD27$^-$CD28$^-$CD4$^+$ T cells treated with A-769662 (AMPK act; 150 μM, 48 h). Data are pooled from 4 independent experiments with 4 individual donors (**a**–**c**) or 3 independent experiments (**d**–**f**) and presented relative to those of cells transfected or transduced with siCtrl or shCtrl, set as 1. ns, not significant, $^{**}P < 0.01$, $^{***}P < 0.001$, ANOVA for repeated measures with Bonferroni post-test correction. Error bars indicate s.e.m. MFI, mean fluorescence intensity.

However, inhibition of p38, but not of Jnk or Erk, enhanced telomerase activity in CD3- and rhIL-2-activated CD27$^-$CD28$^-$CD4$^+$ T cells compared to DMSO (**Fig. 4a**), as previously reported[4,5,30]. Conversely, blocking Erk but not p38 or Jnk activation decreased endogenous DNA damage foci in CD3- and rhIL-2-activated CD27$^-$CD28$^-$CD4$^+$ T cells (**Fig. 4b**). Finally, blocking activation of Jnk, but not of p38 or Erk, restored expression of the key TCR signalosome component Lck in CD27$^-$CD28$^-$CD4$^+$ T cells (**Fig. 4c**) and of the costimulatory receptor CD28 (data not shown). Similar results were obtained in CD27$^-$CD28$^-$CD4$^+$ T cells after siRNA-mediated silencing of Jnk, Erk or p38 (**Supplementary Fig. 4c**,**d**). Thus, MAPK activation promotes T cell senescence, but each MAPK regulates unique functional hallmarks of the senescence program.

We incubated shSesn2-transduced CD27$^-$CD28$^-$CD4$^+$ T cells with the AMPK agonist A-769662, which activates AMPK independently of sestrins (**Supplementary Fig. 4e**) followed by treatment with siRNAs specific for Erk, p38 or Jnk for 48 h. Compared to controls, shSesn2-transduction in CD27$^-$CD28$^-$CD4$^+$ T cells led to enhanced telomerase activity (**Fig. 4d**) and T cell activation (as measured by increased calcium flux) (**Fig. 4e**) and decreased formation of DNA damage foci (**Fig. 4f**). However, agonist-induced activation of AMPK reversed these functional changes (**Fig. 4d**–**f**), suggesting that the sestrins act via AMPK to inhibit functional responses in CD27$^-$CD28$^-$CD4$^+$ T cells. Notably, transfection of siRNA against p38, Jnk or Erk in AMPK agonist–treated, shSesn2-transduced CD27$^-$CD28$^-$CD4$^+$ T cells restored telomerase activity (sip38) and TCR activation (siJnk) and reduced DNA damage foci (siErk) (**Fig. 4d**–**f**). Similar observations were made when silencing sestrin 1 in CD27$^-$CD28$^-$CD4$^+$ T cells (**Supplementary Fig. 4f**). Thus, each MAPK in the sMAC controlled different aspects of T cell senescence downstream of a common sestrin trigger.

Enhanced sMAC formation with age

We investigated whether the sestrins 'preferentially' modulate T cell function in older humans. We found up to a tenfold increase in sestrin expression in total CD4$^+$ T cells from older humans (age 70–85 years) compared to younger ones (age 20–35 years) (**Fig. 5a**). Sestrin 2 expression was highest in CD27$^-$CD28$^-$CD4$^+$ T cells from older individuals (**Fig. 5b**). We did not detect sMAC in CD27$^+$CD28$^+$CD4$^+$ T cells from younger individuals by ImageStream analysis (**Fig. 5c**), whereas sestrin 2 colocalized with phosphorylated Erk, Jnk and p38 in CD27$^-$CD28$^-$CD4$^+$ T cells isolated from the same subjects (**Fig. 5c**). In contrast, CD27$^-$CD28$^-$ and, to a lesser extent, CD27$^+$CD28$^+$ CD4$^+$ T cells from older humans showed colocalization of sestrin 2 and

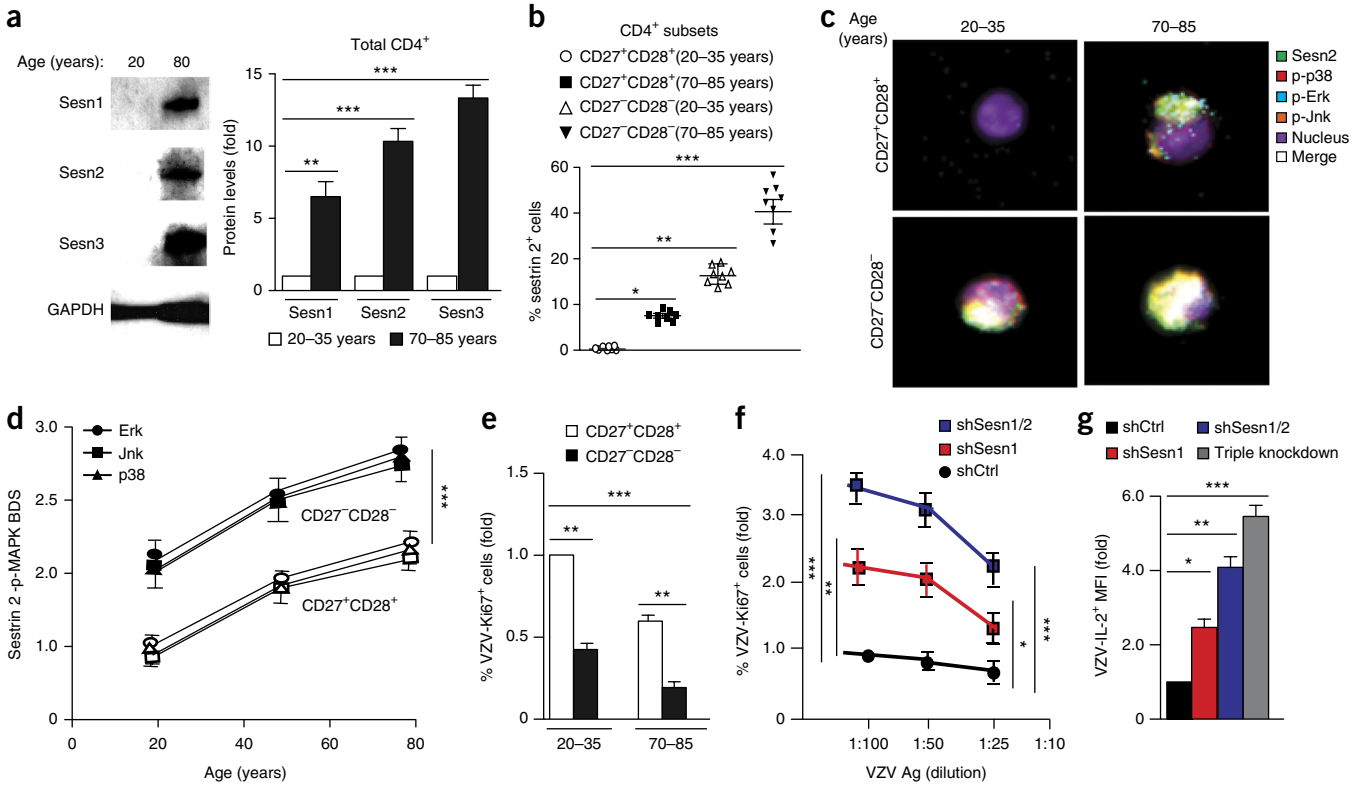

Figure 5 Enhanced sMAC formation with age. (**a**) Immunoblot analysis (left) and quantification (right) of endogenous sestrin proteins (Sesn1–Sesn3) in lysates of primary human CD4+ T cells from young (age 20–35 years) and old (age 70–85 years) individuals. Age-dependent expression of sestrins was normalized to endogenous GAPDH and presented relative to that of young donors, set as 1. (**b**) Flow cytometry analysis of sestrin 2+ cells among CD27+CD28+CD4+ and CD27−CD28−CD4+ T cell subsets from 8 young and 8 old individuals. (**c**) Age-dependent sMAC formation determined by ImageStream in cells as in **b**; representative of 10–20 images from 4 individuals per age group. (**d**) Sestrin 2 and p-MAPK colocalization scores (BDS) of cells as in **c** ($n = 4$ individuals per group). (**e**) Varicella zoster virus (VZV)-specific proliferation in CD27+CD28+CD4+ T and CD27−CD28−CD4+ T cells from 3 young and 3 old donors. Pooled data ($n = 3$) are presented relative to those of CD27+CD28+CD4+ T cells from young donors, set as 1. (**f**) Restored VZV-specific sensitivity (proliferation) in CD27−CD28−CD4+ T cells from old humans after shRNA-mediated knockdown of sestrin 1 only (shSesn1) or sestrin 1 and sestrin 2 (shSesn1/2) ($n = 3$), presented relative to that of cells transduced with shCtrl and stimulated with the lowest VZV antigen (VZV Ag) dilution (1:100), set as 1. (**g**) Restored IL-2 synthesis in sestrin-knockdown CD27−CD28−CD4+ T cells reactivated with autologous APCs loaded with a VZV antigen dilution of 1:100 and presented as in **f** ($n = 3$). Data are pooled from 3 experiments with 3 separate donors (**a**,**e**–**g**) or 4 experiments with 8 (**b**) or 4 (**c**, **d**) donors. $^*P < 0.05$, $^{**}P < 0.01$, $^{***}P < 0.001$, ANOVA for repeated measures with Bonferroni post-test correction. Error bars indicate s.e.m. MFI, mean fluorescence intensity. Uncropped blots are shown in **Supplementary Figure 8**.

phosphorylated MAPKs (**Fig. 5c**). Single-cell analysis of colocalization scores of sestrin 2 and phosphorylated MAPKs showed an age-dependent increase in sMAC formation (**Fig. 5d**). This identifies enhanced formation of the sMAC in human T cells during aging.

Shingles is caused by the reactivation of varicella zoster virus (VZV), and the incidence of this disease increases with age[31,32]. In both young (20–35 years old) and old (70–85 years old) individuals, the CD27+CD28+CD4+ T cells showed higher proliferative activity in response to VZV antigen activation than the CD27−CD28−CD4+ T cell population (**Fig. 5e**). In addition, the proliferation of both subsets was lower in old than in young individuals (**Fig. 5e**). shRNA-mediated silencing of sestrin 1 in CD27−CD28−CD4+ T cells from old donors significantly enhanced their proliferation (**Fig. 5f**) and IL-2 synthesis (**Fig. 5g**) after VZV activation compared to shCtrl transduction, especially at low antigen doses and when transducing shSesn2 and shSesn3 in addition to shSesn1 (**Fig. 5f,g**). Similar results were obtained with cytomegalovirus (CMV)-specific T cell responses from old humans (**Supplementary Fig. 5a,b**). Therefore, silencing of sestrin expression in primary T cell populations from old humans enhanced antigen-specific proliferation and cytokine production *in vitro*.

Sestrin deficiency enhances vaccine response in old mice

CD4+ T cells from 20-month-old mice showed higher expression of sestrin 1, sestrin 2 and sestrin 3 than those from young (2-month-old) mice (**Supplementary Fig. 6a**). We investigated the response to influenza vaccination in age-matched *Sesn1*$^{+/-}$ and *Sesn1*$^{-/-}$ mice. *Sesn1*$^{-/-}$ mice did not express sestrin 1 (**Supplementary Fig. 6b**). Mice were housed together for 20 months and challenged subcutaneously with FLUAD, a clinically approved trivalent inactivated influenza human vaccine that is also effective in rodents[33]. Saline injection served as a control. Five days after vaccination, *Sesn1*$^{-/-}$ but not *Sesn1*$^{+/-}$ mice showed splenomegaly (**Supplementary Fig. 6c**) and a threefold increase in splenocytes (**Fig. 6a**). Correspondingly, we observed a twofold increase in the frequencies of splenic CD4+ and CD8+ T cells in vaccinated *Sesn1*$^{-/-}$ mice, as compared to vaccinated *Sesn1*$^{+/-}$ mice (**Fig. 6b** and **Supplementary Fig. 6d**). The frequencies of myeloid and natural killer (NK) cells were also fivefold and twofold higher, respectively, in vaccinated *Sesn1*$^{-/-}$ mice than in controls (**Supplementary Fig. 6e**,**f**). Within the CD4+ T cell compartment, we observed a twofold expansion of CD62L−CD44+ T effector cells and a corresponding contraction of the CD62L+CD44− naive T cell population from vaccinated *Sesn1*$^{-/-}$ mice, as compared to vaccinated

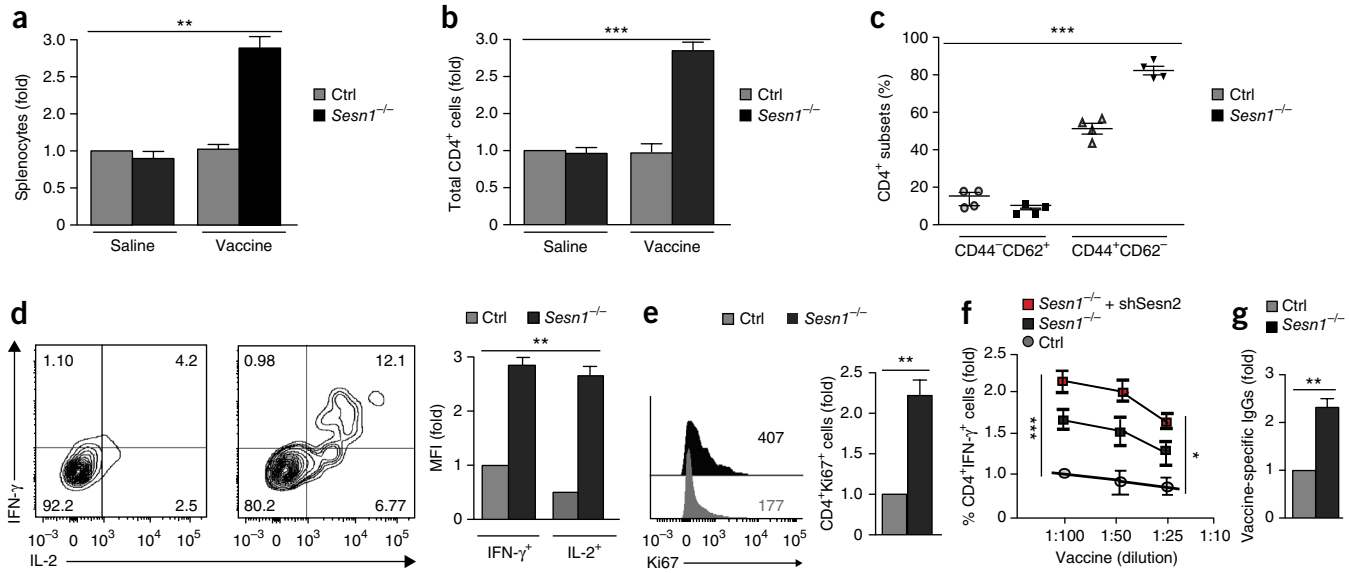

Figure 6 Sestrin deficiency enhances responsiveness to vaccination in old mice. (**a**) Splenocyte count of 20-month-old *Sesn1*$^{+/-}$ and *Sesn1*$^{-/-}$ mice vaccinated with FLUAD (1:20 of human dose) or vehicle saline solution and culled 5 d later. (**b**) Absolute CD4$^+$ T cell count in mice as in **a**. (**c**) Frequencies of naive CD62L$^+$CD44$^-$ and effector CD62L$^-$CD44$^+$ CD4$^+$ T cells in *Sesn1*$^{+/-}$ and *Sesn1*$^{-/-}$ mice vaccinated with FLUAD. (**d**) Counter-plots (left) and mean fluorescence intensity (MFI) data (right) showing IFN-γ and IL-2 production among CD4$^+$ T cells from *Sesn1*$^{+/-}$ and *Sesn1*$^{-/-}$ mice after FLUAD vaccination. Pooled results ($n = 4$) are presented relative to those of vaccinated *Sesn1*$^{+/-}$ mice, set as 1. (**e**) Proliferation among CD4$^+$ T cells from mice as in **d**, representative overlay and pooled data ($n = 4$). Numbers in quadrants indicate cell percentage (**d**) or MFI (**e**). (**f**) IFN-γ production in *Sesn1*$^{+/-}$ and *Sesn1*$^{-/-}$ CD4$^+$ T cells after FLUAD vaccination, transfected or not with shSesn2 and restimulated for 18 h with *Sesn1*$^{+/-}$ APCs pre-loaded with various dilutions of FLUAD. Results are presented relative to that of vaccinated *Sesn1*$^{+/-}$ mice, set as 1. (**g**) 1-week vaccine-specific IgG titers in serum of vaccinated *Sesn1*$^{+/-}$ or *Sesn1*$^{-/-}$ mice. ELISA-based binding assays are presented relative to those of vaccinated *Sesn1*$^{+/-}$ mice, set as 1. Data are from 2 experiments with 6 (**a**,**b**) or 4 (**c**–**e**,**g**) individual aged-matched mice per group or 3 independent experiments with 3 individual mice per group (**f**). $^*P < 0.05$, $^{**}P < 0.01$, $^{***}P < 0.001$, ANOVA for repeated measures with Bonferroni post-test correction (**a**–**c**,**f**) or paired Student's *t*-test (**d**,**e**,**g**). Error bars indicate s.e.m.

Sesn1$^{+/-}$ controls (**Fig. 6c** and **Supplementary Fig. 6g**). These differences in T cell frequencies between genotypes were not evident before vaccination (data not shown). Functionally, *Sesn1*$^{-/-}$ CD4$^+$ T cells showed higher IL-2 and IFN-γ production and enhanced proliferation than *Sesn1*$^{+/-}$ mice after vaccination (**Fig. 6d,e**). Therefore, sestrin deficiency enhances T cell responsiveness and expansion of innate cells during aging *in vivo*.

To investigate whether enhanced T cell responsiveness after vaccination was antigen specific, we re-challenged *Sesn1*$^{+/-}$ and *Sesn1*$^{-/-}$ T cells with *Sesn1*$^{+/-}$ antigen-presenting cells (APCs) pulsed with FLUAD *in vitro*. We observed higher IFN-γ and IL-2 expression in *Sesn1*$^{-/-}$ than in *Sesn1*$^{+/-}$ CD4$^+$ T cells (**Fig. 6f** and data not shown). In addition, siRNA-mediated silencing of sestrin 2 in *Sesn1*$^{-/-}$ CD4$^+$ T cells further increased their responsiveness to *Sesn1*$^{+/-}$ APCs pulsed with FLUAD (**Fig. 6f**).

When measuring antibody titers, we found a two- to threefold increase in influenza-specific circulating IgGs in *Sesn1*$^{-/-}$ mice, compared to *Sesn1*$^{+/-}$ mice (**Fig. 6g**) and *Sesn1*$^{-/-}$ B cells showed enhanced IgG isotypic switching compared to *Sesn1*$^{+/-}$ mice after vaccination (**Supplementary Fig. 6h**). B cell frequencies, however, were slightly lower in the spleens of vaccinated *Sesn1*$^{-/-}$ mice than in those of vaccinated *Sesn1*$^{+/-}$ mice (data not shown). Vaccination increased the numbers of T cells, NK and myeloid cells and IgG$^+$ B cells in *Sesn1*$^{-/-}$ mice, as compared to unvaccinated *Sesn1*$^{-/-}$ mice (**Supplementary Fig. 6i**). Thus, sestrin deficiency restores vaccine responsiveness during aging *in vivo*.

MAPK inhibition phenocopies sestrin deficiency *in vivo*

We next measured Erk, Jnk and p38 phosphorylation in sestrin 2$^+$ CD4$^+$ T cells, which made up as much as 70% of the total CD4$^+$ T cell pool (**Fig. 7a**) in 20-month-old *Sesn1*$^{+/-}$ and *Sesn1*$^{-/-}$ mice after FLUAD vaccination. Erk, Jnk and p38 phosphorylation was robust in sestrin 2$^+$ CD4$^+$ T cells from *Sesn1*$^{+/-}$ mice and was low in *Sesn1*$^{-/-}$ CD4$^+$ T cells (**Fig. 7b**). Notably, disruption of Erk, Jnk and p38 phosphorylation was correlated with higher IFN-γ production in sestrin 2$^+$ CD4$^+$ T cells from vaccinated *Sesn1*$^{-/-}$ mice than in *Sesn1*$^{+/-}$ mice (**Fig. 7c**). Sestrin 1 deficiency did not inhibit Erk, Jnk or p38 phosphorylation in the minor sestrin 2$^-$ CD4$^+$ T cells compared to those from *Sesn1*$^{+/-}$ mice (**Supplementary Fig. 7a**). To test whether inhibition of all MAPKs would boost vaccine responsiveness in aged mice, we administered the Erk inhibitor FR18024, the Jnk inhibitor SP-600125 and/or the p38 inhibitor SB-203580 by intraperitoneal injection in 16-month-old mice vaccinated with FLUAD and examined both the sestrin 2$^+$ CD4$^+$ T cell and CD19$^+$ B cell subsets. Mice treated with all three MAPK inhibitors developed splenomegaly (**Fig. 7d** and **Supplementary Fig. 7b**) and showed higher splenic CD4$^+$ T cell numbers than did DMSO vehicle–treated controls or mice receiving only one MAPK inhibitor after vaccination (**Fig. 7e**). MAPK self-phosphorylation was either selectively or globally inhibited in CD4$^+$ T cells from mice treated with one or all three MAPK inhibitors, respectively, as compared to mice treated with DMSO (**Fig. 7f**). Compared to DMSO treatment, triple (but not single) inhibition of MAPKs boosted IFN-γ synthesis in sestrin 2$^+$ CD4$^+$ T cells after vaccination (**Fig. 7g**). Triple MAPK inhibition also induced a threefold increase in the frequencies of sestrin 2$^+$ CD19$^+$ B cells undergoing vaccine-specific IgG isotypic switch, which was not observed with inhibition of individual MAPKs (**Fig. 7g**). In contrast, inhibition of MAPK signaling in both sestrin 2$^-$ CD4$^+$ T and CD19$^+$ B cells reduced vaccine-induced IFN-γ production and IgG isotype switching, respectively (**Supplementary Fig. 7c**).

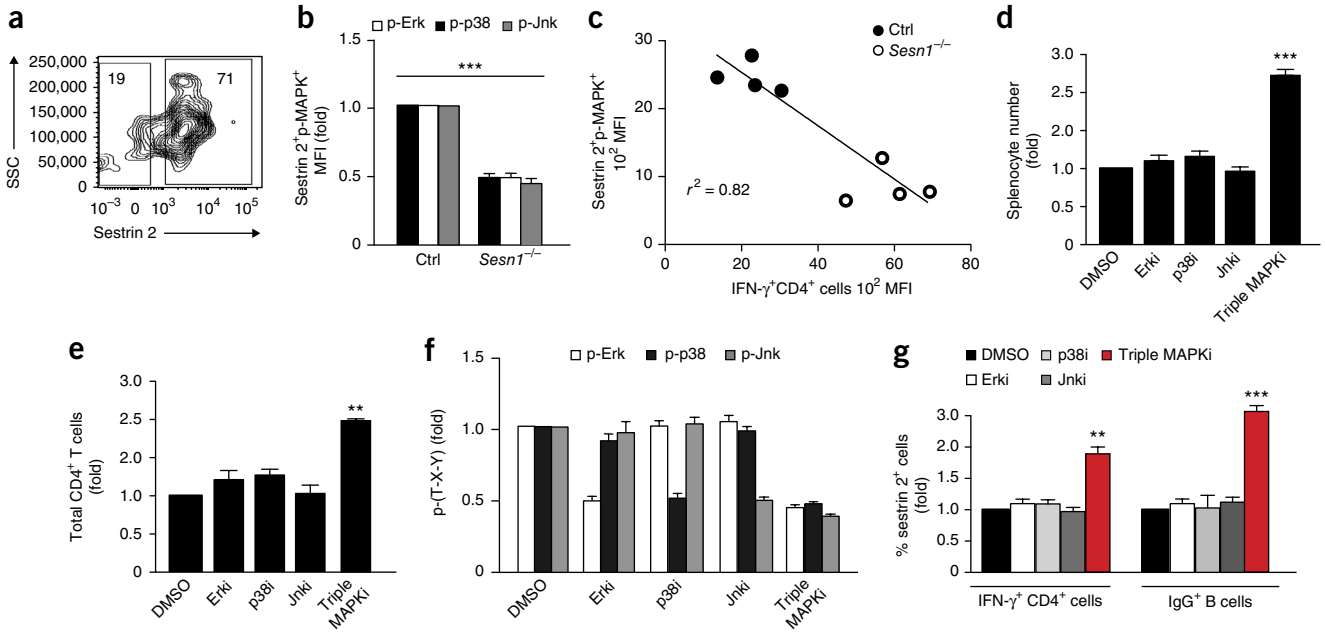

Figure 7 Simultaneous MAPK inhibition phenocopies sestrin deficiency *in vivo*. (**a**) Phospho-flow analysis of sestrin 2 expression in CD4+ T cells from 16-month-old mice. Numbers in quadrants indicate cell percentages. (**b**) Erk, Jnk and p38 phosphorylation (p-) in CD4+ T cells from control *Sesn1*$^{+/-}$ and *Sesn1*$^{-/-}$ mice (20-months old) vaccinated as in **Figure 6**. Data ($n = 4$) are presented relative to those of control *Sesn1*$^{+/-}$ mice, set as 1. (**c**) Correlation between reduced sestrin 2–p-Erk–p-Jnk–p-p38 signaling and enhanced IFN-γ production in CD4+ T cells from *Sesn1*$^{+/-}$ and *Sesn1*$^{-/-}$ mice after FLUAD vaccination ($n = 4$; $r^2 = 0.82$). (**d**,**e**) Splenocyte (**d**) and CD4+ T cell counts (**e**) from 16-old-mice injected with Erk inhibitor (Erki, 25 mg/kg), Jnk inhibitor (Jnki, 16 mg/kg) and p38 inhibitor (p38i, 10 mg/kg) individually or together (triple MAPKi), vaccinated with FLUAD and injected daily with inhibitors for 5 d. Results are presented relative to those in DMSO-treated mice, set as 1. (**f**) MAPK self-phosphorylation in CD4+ T cells from mice as in **d** and **e** assessed by *in vitro* kinase assays and presented relative to those of DMSO-treated mice, set as 1. (**g**) FLUAD-driven IFN-γ production and IgG isotypic switch in sestrin 2+CD4+ T and CD19+ B cells in mice as in **d** and **e**, assessed by flow cytometry. Pooled data ($n = 4$) are presented relative to those of DMSO treated mice, set as 1. Data are pooled from 4 experiments with 4 (age-matched) mice per group (**a**–**e**,**g**) or 2 experiments (**f**). $^{**}P < 0.01$, $^{***}P < 0.001$, ANOVA for repeated measures with Bonferroni post-test correction. Error bars indicate s.e.m. MFI, mean fluorescence intensity.

Thus, disruption of all MAPK pathways in sestrin 2+ T and B cell populations enhanced vaccine responsiveness in old mice.

The sMAC is formed in mouse T cells

We isolated CD4+ T cells from *Sesn1*$^{+/-}$ and *Sesn1*$^{-/-}$ mice, immunoprecipitated sestrin 2, and investigated Erk, Jnk and p38 phosphorylation. Sestrin 2 complexes from *Sesn1*$^{-/-}$ CD4+ T cells showed lower phosphorylation of Erk, Jnk and p38 than those from *Sesn1*$^{+/-}$ CD4+ T cells (**Fig. 8a**,**b**). Sestrin 2–MAPK binding was not affected by sestrin 1 deficiency (data not shown). ImageStream analysis confirmed disrupted sMAC activation in spleen-derived CD4+ T cells from *Sesn1*$^{-/-}$ mice compared to *Sesn1*$^{+/-}$ mice (**Fig. 8c**,**d**). *In vitro* kinase assays showed that incubation of sestrin 2 immunoprecipitates from *Sesn1*$^{-/-}$ mouse CD4+ T cells with recombinant human sestrin 1 restored MAPK activation in lysates from these cells (**Fig. 8e**). This effect was not observed in sestrin 2 immunoprecipitates from CD4+ T cells treated with siAMPK-γ (**Fig. 8e**). A-769662 agonist–driven activation of AMPK also restored MAPK phosphorylation in sestrin 2 immunoprecipitates from splenic *Sesn1*$^{-/-}$ CD4+ T cells and was further enhanced by the addition of ATP, which is needed to fuel MAPK autophosphorylation (**Fig. 8f**). Thus, the sMAC is formed and coordinated by the sestrins in mice.

DISCUSSION

Here we show that in CD27−CD28−CD4+ T cells Erk, Jnk and p38 MAPK are simultaneously activated owing to constitutive expression of sestrin proteins. In flies, sestrin expression increases on maturation and aging and triggers feedback anti-aging pathways through a TORC1 inhibitory complex[20]. Similarly, in muscle, sestrins exhibit mTORC1-dependent anti-aging activities[22]. We now describe an opposite pro-aging function of sestrins in T cells that occurs independently of mTORC1 and instead is mediated by an Erk–Jnk–p38 activation complex, termed sMAC. Such coordinated MAPK activation was previously unknown and is distinct from the canonical MAPK activation cascades where Erk, Jnk and p38 are regulated independently[11].

All regulatory elements within the sMAC interacted constitutively in CD27−CD28−CD4+ T cells. The sMAC was also distinct from the previously described sestrin–mTORC1 inhibitory complexes containing GATOR and RAG proteins[23–25], suggesting that the anti-aging–pro-aging dichotomy of sestrin action in T cells versus other cell types may depend on different sestrin–protein interactions. Consistently, mTORC1 inhibition has been strongly associated with longevity in both murine muscle and in insects[34], and p38 MAPK activation can drive T cell aging and senescence[4–6,30]. Sestrin may therefore exert anti- or pro-aging effects through different macromolecular complexes. Whether the sMAC also controls aging in nonimmune cells remains to be determined.

The sMAC also formed in CD27+CD28+ T cells upon glucose deprivation (data not shown), and this extends previous observations highlighting the convergence of senescence and low-nutrient signals to regulate T cell function ('intra-sensory' signaling)[5,9]. When examining glucose-deprived sestrin-silenced CD27+CD28+ T cells, we also found disruption of AMPK phosphorylation and a transient

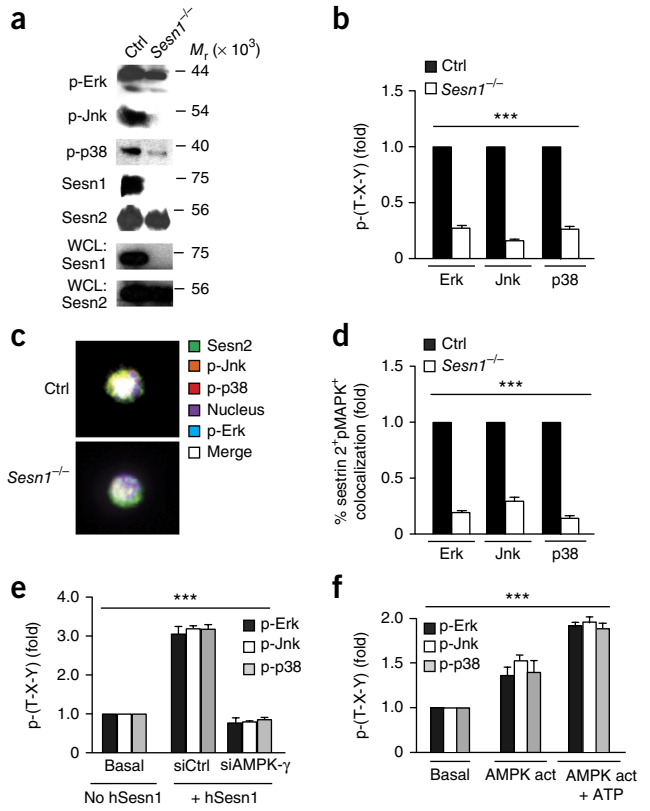

Figure 8 The sMAC is formed in mouse T cells. (**a**,**b**) Immunoblot analysis (**a**) and quantification (**b**) of phosphorylated (p-) Erk, Jnk and p38 in lysates from CD4+ T cells from 20-month-old vaccinated *Sesn1*$^{+/-}$ and *Sesn1*$^{-/-}$ mice after immunoprecipitation with antibodies to sestrin 2 (Sesn2). Results in **b** are presented relative to those in *Sesn1*$^{+/-}$ mice, set as 1. Sestrin 2 expression in whole cell lysates (WCL) served as loading control. Sestrin 1 expression is also shown. (**c**,**d**) ImageStream analysis (**c**) and percentage of colocalization (**d**) of sestrin 2+pMAPK+ CD4+ T cells from *Sesn1*$^{+/-}$ and *Sesn1*$^{-/-}$ mice, 5 d after vaccination with FLUAD, presented as in **b**. (**e**,**f**) *In vitro* MAPK assays of sestrin 2 immunoprecipitates from mouse *Sesn1*$^{-/-}$ CD4+ T cells incubated for 60 min with (hSesn1) or without (no hSesn1) recombinant human sestrin 1 (**e**) or the AMPK agonist A-769662 in the presence or absence of ATP (**f**). Results are presented relative to that of nonreconstituted *Sesn1*$^{-/-}$ cells (basal), set as 1. In **e**, cells were transfected with siRNAs 48 h before lysis. Data are representative of 4 experiments (**a**,**c**) or pooled from 4 experiments with 4 (age-matched) individual mice (**b**,**d**–**f**). $^{**}P < 0.01$, $^{***}P < 0.001$, ANOVA for repeated measures with Bonferroni post-test correction. Error bars indicate s.e.m. Uncropped blots are shown in **Supplementary Figure 8**.

increase in T cell activation followed by T cell death when glucose deprivation persisted (data not shown). Sestrins may thus function as energy-sensing 'rheostats' that directly bind AMPK-γ and promote AMPK activation to favor T cell survival at the expenses of function under severe stress.

The sMAC was larger than the sestrin–mTORC1 inhibitory complex, and additional proteins may contribute to its regulation. p38 autophosphorylation is a feature of noncanonical MAPK activation in T cells that requires p38 binding to specific scaffolding molecules such as TAB1 (refs. 5,35). We now show that sMAC coordinates the simultaneous activation of all MAPK pathways. However, TAB1 was not required for the activation of Jnk or Erk, but it mediated activation of p38 within the sMAC (data not shown). We propose a model in which three separate MAPK subcomplexes are constitutively bound to AMPK in their inactive forms. When expressed, sestrins promote the unloading of ATP from AMPK-γ and activate the AMPK complex. In turn, this triggers the autophosphorylation of all associated MAPKs. Distinct scaffolding molecules may be required to support the autophosphorylation of each of the three MAPKs in the sMAC.

Silencing of sestrin expression allowed a broad enhancement of T cell activity, whereas downstream targeting of any individual MAPK was much more selective. It is therefore possible to exert narrower or broader control over senescence-related T cell functional changes by targeting different molecules within the sMAC. As each MAPK controls different aspects of T cell senescence, they may have to be targeted simultaneously for effective immune boosting during aging. However, direct inhibition of MAPKs may not be feasible for immunotherapy, as it would negatively regulate the responses of T and B lymphocytes that do not express sestrins. In contrast, inhibition of the sestrins would disrupt global MAPK signaling. This would spare sestrin-negative cells in which MAPKs may be activated via canonical pathways[36] and may thus circumvent toxicity. A possible caveat is that sestrin inhibition may enhance the proliferative activity of senescent cells that have residual DNA damage and, therefore, prolonged inhibition of sestrins may result in malignancy[37]. However, short-term inhibition of sestrins could be a beneficial immunotherapeutic strategy.

METHODS

Methods, including statements of data availability and any associated accession codes and references, are available in the online version of the paper.

Note: Any Supplementary Information and Source Data files are available in the online version of the paper.

ACKNOWLEDGMENTS

We thank A. Sewell, D. Mosser and O. Franzese for discussions. Supported by the Wellcome Trust (AZR00630 to A.L.) and the Biotechnology and Biological Science Research Council (BB/L005328/1 to A.N.A.). D.C.O.G. was supported by the Coordination for the Improvement of Higher Education Personnel (CAPES-Brazil) (grant number 99999.006198/2014-07). B.M.-D. was supported by the Swiss National Foundation (P300PB_161092 and P2BSP3_151877); T.M.D. was supported by an NIHR BRC grant; D.E. was supported by a Miguel Servet Fellowship (CP12/03114) and a FIS project (PI14/00579) from the Instituto de Salud Carlos III, Spain. Mouse Sestrin 1 studies were supported by the Ellison Medical Foundation (AG-SS-2440-10 to M.K.) and the NIH (R21AG045432 to J.H.L.). A.L. is a recipient of a Sir Henry Wellcome Trust Fellowship sponsored by M.L. Dustin (University of Oxford).

AUTHOR CONTRIBUTIONS

A.L. conceived, planned and performed the study, analyzed and interpreted data and wrote the paper; D.C.O.G., B.M.-D. and T.M. performed experiments; D.E. provided lentiviral tools; D.W.G. supported mouse experiments; J.H.L. and M.K. provided *Sesn1*$^{-/-}$ mice and experimental advice and edited the paper; A.N.A. provided overall guidance, experimental advice and laboratory infrastructure and edited the paper; all authors read and approved the final manuscript.

COMPETING FINANCIAL INTERESTS

The authors declare competing financial interests: details are available in the online version of the paper.

1. Montecino-Rodriguez, E., Berent-Maoz, B. & Dorshkind, K. Causes, consequences, and reversal of immune system aging. *J. Clin. Invest.* **123**, 958–965 (2013).
2. Dorshkind, K., Montecino-Rodriguez, E. & Signer, R.A.J. The ageing immune system: is it ever too old to become young again? *Nat. Rev. Immunol.* **9**, 57–62 (2009).
3. Lutz, W., Sanderson, W. & Scherbov, S. The coming acceleration of global population ageing. *Nature* **451**, 716–719 (2008).
4. Di Mitri, D. *et al.* Reversible senescence in human CD4+CD45RA+CD27− memory T cells. *J. Immunol.* **187**, 2093–2100 (2011).

5. Lanna, A., Henson, S.M., Escors, D. & Akbar, A.N. The kinase p38 activated by the metabolic regulator AMPK and scaffold TAB1 drives the senescence of human T cells. *Nat. Immunol.* **15**, 965–972 (2014).
6. Henson, S.M. *et al.* p38 signaling inhibits mTORC1-independent autophagy in senescent human CD8$^+$ T cells. *J. Clin. Invest.* **124**, 4004–4016 (2014).
7. Li, G. *et al.* Decline in miR-181a expression with age impairs T cell receptor sensitivity by increasing DUSP6 activity. *Nat. Med.* **18**, 1518–1524 (2012).
8. Müller-Durovic, B. *et al.* Killer cell lectin-like receptor G1 inhibits NK cell function through activation of adenosine 5′-monophosphate-activated protein kinase. *J. Immunol.* **197**, 2891–2899 (2016).
9. Akbar, A.N., Henson, S.M. & Lanna, A. Senescence of T lymphocytes: implications for enhancing human immunity. *Trends Immunol.* **37**, 866–876 (2016).
10. Weng, N.-P., Akbar, A.N. & Goronzy, J. CD28$^-$ T cells: their role in the age-associated decline of immune function. *Trends Immunol.* **30**, 306–312 (2009).
11. Chang, L. & Karin, M. Mammalian MAP kinase signalling cascades. *Nature* **410**, 37–40 (2001).
12. Johnson, G.L. & Lapadat, R. Mitogen-activated protein kinase pathways mediated by ERK, Jnk, and p38 protein kinases. *Science* **298**, 1911–1912 (2002).
13. Liu, Y., Shepherd, E.G. & Nelin, L.D. MAPK phosphatases—regulating the immune response. *Nat. Rev. Immunol.* **7**, 202–212 (2007).
14. Chen, R.E. & Thorner, J. Function and regulation in MAPK signaling pathways: lessons learned from the yeast *Saccharomyces cerevisiae*. *Biochim. Biophys. Acta* **1773**, 1311–1340 (2007).
15. Budanov, A.V. *et al.* Identification of a novel stress-responsive gene Hi95 involved in regulation of cell viability. *Oncogene* **21**, 6017–6031 (2002).
16. Peeters, H. *et al.* PA26 is a candidate gene for heterotaxia in humans: identification of a novel PA26-related gene family in human and mouse. *Hum. Genet.* **112**, 573–580 (2003).
17. Velasco-Miguel, S. *et al.* PA26, a novel target of the p53 tumor suppressor and member of the GADD family of DNA damage and growth arrest inducible genes. *Oncogene* **18**, 127–137 (1999).
18. Budanov, A.V. & Karin, M. p53 target genes sestrin1 and sestrin2 connect genotoxic stress and mTOR signaling. *Cell* **134**, 451–460 (2008).
19. Hardie, D.G., Ross, F.A. & Hawley, S.A. AMPK: a nutrient and energy sensor that maintains energy homeostasis. *Nat. Rev. Mol. Cell Biol.* **13**, 251–262 (2012).
20. Lee, J.H. *et al.* Sestrin as a feedback inhibitor of TOR that prevents age-related pathologies. *Science* **327**, 1223–1228 (2010).
21. Lee, J.H. *et al.* Maintenance of metabolic homeostasis by Sestrin2 and Sestrin3. *Cell Metab.* **16**, 311–321 (2012).
22. Lee, J.H., Budanov, A.V. & Karin, M. Sestrins orchestrate cellular metabolism to attenuate aging. *Cell Metab.* **18**, 792–801 (2013).
23. Parmigiani, A. *et al.* Sestrins inhibit mTORC1 kinase activation through the GATOR complex. *Cell Rep.* **9**, 1281–1291 (2014).
24. Peng, M., Yin, N. & Li, M.O. Sestrins function as guanine nucleotide dissociation inhibitors for Rag GTPases to control mTORC1 signaling. *Cell* **159**, 122–133 (2014).
25. Chantranupong, L. *et al.* The sestrins interact with GATOR2 to negatively regulate the amino-acid-sensing pathway upstream of mTORC1. *Cell Rep.* **9**, 1–8 (2014).
26. Yang, Y.-L. *et al.* SESN-1 is a positive regulator of lifespan in *Caenorhabditis elegans*. *Exp. Gerontol.* **48**, 371–379 (2013).
27. Chen, C.C. *et al.* FoxOs inhibit mTORC1 and activate Akt by inducing the expression of Sestrin3 and Rictor. *Dev. Cell* **18**, 592–604 (2010).
28. Hay, N. p53 strikes mTORC1 by employing sestrins. *Cell Metab.* **8**, 184–185 (2008).
29. Göransson, O. *et al.* Mechanism of action of A-769662, a valuable tool for activation of AMP-activated protein kinase. *J. Biol. Chem.* **282**, 32549–32560 (2007).
30. Lanna, A. *et al.* IFN-α inhibits telomerase in human CD8$^+$ T cells by both hTERT downregulation and induction of p38 MAPK signaling. *J. Immunol.* **191**, 3744–3752 (2013).
31. Oxman, M.N. *et al.* A vaccine to prevent herpes zoster and postherpetic neuralgia in older adults. *N. Engl. J. Med.* **352**, 2271–2284 (2005).
32. Levin, M.J. Immune senescence and vaccines to prevent herpes zoster in older persons. *Curr. Opin. Immunol.* **24**, 494–500 (2012).
33. Oh, J.Z. *et al.* TLR5-mediated sensing of gut microbiota is necessary for antibody responses to seasonal influenza vaccination. *Immunity* **41**, 478–492 (2014).
34. Johnson, S.C., Rabinovitch, P.S. & Kaeberlein, M. mTOR is a key modulator of ageing and age-related disease. *Nature* **493**, 338–345 (2013).
35. Round, J.L. *et al.* Scaffold protein Dlgh1 coordinates alternative p38 kinase activation, directing T cell receptor signals toward NFAT but not NF-kappaB transcription factors. *Nat. Immunol.* **8**, 154–161 (2007).
36. Ashwell, J.D. The many paths to p38 mitogen-activated protein kinase activation in the immune system. *Nat. Rev. Immunol.* **6**, 532–540 (2006).
37. Akbar, A.N. & Henson, S.M. Are senescence and exhaustion intertwined or unrelated processes that compromise immunity? *Nat. Rev. Immunol.* **11**, 289–295 (2011).

ONLINE METHODS

Human studies. We collected heparinized peripheral blood samples from 120 individuals (aged 20–85 years, male 55% and female 45%). Samples from young (aged 20–35 years) and old (aged 65–80 years) donors were obtained with the approval of the Ethical Committee of Royal Free and University College Medical School and with voluntary informed consent, in accordance with the Declaration of Helsinki. Donors did not have any comorbidities, were not on any immunosuppressive drugs, and retained physical mobility and lifestyle independence.

Western blot analysis. Lysates from 2×10^6 cells were used for western blot analysis. Endogenous signaling studies were assessed in *ex vivo* purified $CD4^+$ CD27 and CD28 T cell subsets as described previously[5]. Transduced $CD27^-CD28^-CD4^+$ T cells were analyzed by immunoblotting 1 week after activation (described below). Membranes were probed with antibodies to sestrin 1 (Genetex GTX118141; Abcam EPR1930(2)), sestrin 2 (Cell Signaling (D1B6) 8487), sestrin 3 (Sigma-Aldrich HPA037935), Erk, phosphorylated (p-)Erk (9101), p-Jnk ((81E11) 4668), p-p38 (9211), AMPK-α (2532), p-AMPK-α ((40H9) 2535), μ (2972), S6K1 ((49D7) 2708), MKK7 (4172), MKK4 (9152), p-MEK1/2 (9121) and GAPDH ((14C10) 2118) (all from Cell Signaling).

Immunoprecipitation. For coimmunoprecipitation analysis, cell lysates were prepared using ice-cold HNGT buffer (50 mM HEPES, pH 7.5, 150 mM EDTA, 10 mM sodium pyrophosphate, 100 mM sodium orthovanadate, 100 mM sodium fluoride, 10 mg/ml aprotinin, 10 mg/ml leupeptin, and 1 mM phenylmethylsulfonyl fluoride). Lysates from 20×10^6 cells were used for immunoprecipitation analysis. For the minor $CD28^-CD27^-CD4^+$ subset, cells from two separate individuals were pooled to obtain sufficient material for the assay. Extracts were incubated with the indicated antibodies at 4 °C on a rotary shaker overnight, followed by incubation with protein A–G conjugated agarose beads (Santa Cruz Biotechnology) at 4 °C for 3 h. Samples were washed and analyzed by immunoblot as indicated. Coimmunoprecipitated proteins were detected using mouse anti-rabbit IgG conformation-specific (L27A9; Cell Signaling) or mouse anti-rabbit IgG light chain, followed by a secondary anti-mouse IgG antibody (all from Cell Signaling) and ECL Prime Western detection kit (GE Healthcare).

***In vitro* binding assay.** Briefly, lysates from $CD27^+CD28^+CD4^+$ T cells were incubated with recombinant sestrins for 1 h before total AMPK immunoprecipitation. AMPK complexes were washed extensively, and global MAPK activation was measured by immunoblotting or *in vitro* kinase assays (described below). Absolute MAPK binding was determined using ELISA-based total Erk, Jnk and p38 detection assays according to the manufacturer's instructions (Abcam; described below). In some experiments, absolute MAPK binding was determined on endogenous sestrin immunoprecipitates from $CD27^-CD28^-CD4^+$ T cells, 36-48 h after transfection. MAPK binding assays are shown as proportional to fold increase at 450 nm absorbance emission of triplicate wells ± s.e.m., and were normalized to the indicated 'bait' proteins, i.e., sestrin 1 (MBS9327570) or AMPK-α (ab151280) used in the immunoprecipitation assay.

***In vitro* kinase assay.** Sestrin or AMPK immunoprecipitates were washed twice in lysis buffer and twice in kinase buffer (all from Cell Signaling). Kinase reactions were incubated for 30 min at 30 °C either in the absence or in the presence of 200 μM ATP (Cell Signaling), as indicated. MAPK activity was assessed using Phospho-Tracer ELISA Kits according to the manufacturer's instructions (Abcam). In some experiments, exogenous recombinant human sestrin proteins (Genway; 1 μg/mL), the AMPK agonist A-769662 (150 μM), the Erk inhibitor FR18024 (20 μM); the Jnk inhibitor SP-600125 (10 μM); or the p38 inhibitor SB-203580 (10 μM) were added directly to the *in vitro* kinase reaction itself for 30 min as indicated. *In vitro* kinase assays are shown as proportional to fold increase at 450 nm absorbance emission of triplicate wells ± s.e.m., normalized to the total amounts of coimmunoprecipitated MAPKs.

Detection of coimmunoprecipitated proteins by ELISA. Briefly, an antibody mix was prepared by adding Capture Antibody Reagent(s) to MAPKs and Detection Antibody Reagent (both provided with the Phospho Tracer kit by Abcam), in a 1:1 ratio, and 50 μl of this antibody mix were added to the *in vitro* kinase/binding reaction product (50 μl), loaded in the Phospho Tracer microplates. Antibody binding was then allowed for 1 h at room temperature on a microplate shaker. Wells were rinsed three times with 200 μl 1× washing buffer (provided with the kit). Meanwhile, a substrate mix was prepared immediately before use by diluting 1:100 the HR-substrate 10-acetyl-3,7-dihydroxyphenoxazine (ADHP) with ADHP Dilution Buffer (both provided with the kit), a stabilized H_2O_2 solution. Next, 100 μl of this substrate mix were added to each well, and incubated for 10 min at room temperature on a microplate shaker for color development. The reaction of conversion of ADHP into the fluorescent molecule Resorufin was then stopped by adding 10 μl stop solution to each well. Signal was read using an ELISA reader microplate. Background was calculated in parallel IgG control immunoprecipitation reactions.

Measurement of AMPK-γ ATP loading. T cell AMPK-γ1 immunoprecipitates were analyzed for ATP content using an ATP determination kit, according to the manufacturer's instructions (Life Technologies). Total AMPK-γ1 immunoprecipitates were quantified by ELISA (LifeSpan Biosciences).

T cell activation dynamics. For detection of intracellular calcium, we used X-Rhod-1, a visible light–excitable calcium chelator suitable for flow cytometry. Briefly, transduced cells were incubated with this dye (2.5 μM, 37 °C; 20 min) washed in indicator-free medium to eliminate unspecific binding, then incubated for further 30 min to allow complete dye de-esterification, as instructed by the manufacturer (Molecular Probes, Invitrogen). Cells were then stimulated with anti-CD3 for 2 min immediately followed by flow cytometry analysis. In experiments with 'multilayer' modulation of signaling, stably transduced primary human $CD27^-CD28^-CD4^+$ T cells were activated with anti-CD3 (0.5 μg/mL) and rh-IL-2 (10 ng/mL) for 24 h in the presence of siRNAs and/or the AMPK activator A-769662 (150 μM) or the mTORC1 inhibitor rapamycin (20 ng/mL), followed by dye incubation, short-term reactivation and intracellular calcium detection, as above. IL-2 synthesis or release was analyzed by ELISA-based or intracellular flow cytometry respectively, as indicated. Active cycling upon stimulation was further confirmed by staining for the proliferation-related antigen Ki67.

Lentiviral vector design. The pHIV1-SIREN-GFP system used for knockdown of gene expression possesses a U6-shRNA cassette to drive shRNA expression and a GFP reporter gene that is controlled by a PGK promoter[5]. The following siRNA sequences were used for gene knockdowns: CCTAAGGTTAAGTCGCCCTCG (shCTRL), ATGATGTCAGATGGTGAATTT (shAMPK-α), CCAGGACCA ATGGTAGACAAA (shSesn1), CCGAAGAATGTACAACCTCTT (shSesn2) and CAGTTCTCTAGTGTCAAAGTT (shSesn3). The shAMPK-α sequence was previously described and validated in primary human $CD4^+$ T cells[5]. VSV-g pseudotyped lentiviral particles were produced, concentrated and titrated in HEK293 cells as described[38].

Cell cultures and lentiviral transduction of primary human T lymphocytes. Cells were cultured in RPMI-1640 medium supplemented with 10% heat-inactivated FCS, 100 U/ml penicillin, 100 mg/ml streptomycin, 50 μg/ml gentamicin, and 2 mM L-glutamine (all from Invitrogen) at 37 °C in a humidified 5% CO_2 incubator. Purified human highly differentiated $CD27^-CD28^-CD4^+$ T cells were activated in the presence of plate-bound anti-CD3 (purified OKT3, 0.5 μg/ml) plus rhIL-2 (R&D Systems, 10 ng/ml), and then transduced with pHIV1-Siren lentiviral particles (multiplicity of infection (MOI) = 10) at 48 and 72 h after activation. Nonsenescent $CD27^+CD28^+CD4^+$ T cells were cultured and transduced as above after activation by plate-bound anti-CD3 (0.5 μg/mL) plus anti-CD28 (0.5 μg/mL). When antigen-specific responsiveness was assessed, $CD27^-CD28^-CD4^+$ T cells were reactivated 10 d after transduction using autologous antigen-presenting cells (APCs) pre-loaded for 4 h with various dilutions of Varicella zoster or cytomegalovirus lysates (Zeptometrix Corporation), as indicated. APCs were obtained by depleting $CD3^+$ cells from autologous, fresh peripheral blood mononuclear cell (PBMC) preparations and cultured with transduced T cells in a 3:1 ratio. Antigen-specific responses are shown as fold increase normalized to transduced cells before restimulation, with control cells set as 1, in triplicate experiments.

doi:10.1038/ni.3665

Transfections. Human or mouse primary $CD4^+$ T cells were transfected with siRNAs to Erk, Jnk, p38, AMPK-γ, MEKK1, MEKK4, MEKK7 or an irrelevant control siRNA sequence (all from Santa Cruz Biotechnology) using Nucleofector Kit according to the supplier's protocol (Amaxa, Lonza Walkersville; program V024), as indicated. Cells were analyzed 36–48 h later for functional or signaling readouts.

Quantitative PCR (real-time analysis). Four days after transduction, samples from 5×10^5 viable senescent $CD27^-CD28^-CD4^+$ T cells were resuspended in TRIzol (Ambion). For cDNA synthesis, RNA was reverse transcribed using M-MuLV Reverse Transcriptase (New England BioLab) and random primers. Relative transcript expression was normalized using the ΔΔCt threshold cycle method according to the supplier's protocol (Applied Biosystems).

Signaling studies. Cells were fixed with warm Cytofix Buffer (BD Biosciences) at 37 °C for 10 min, permeabilized with ice-cold Perm Buffer III (BD Biosciences) at 4 °C for 30 min and then incubated for 30 min at room temperature with antibodies to: Lck, ZAP-70, p-AMPK, sestrin 2 (all from Cell Signaling), PercPCy5-conjugated p-Erk (612592), Alexa Fluor 647–conjugated p-Jnk (562481), PE-conjugated p-p38 (612565) and PE-conjugated γ-H2A-x (all from BD Biosciences). When primary unconjugated antibodies were used, they were subsequently probed with a secondary mouse (or goat) Alexa Fluor 647–conjugated anti-rabbit IgG (BD Biosciences) for 30 min at room temperature, in the dark. After washing in Stain Buffer (BD Pharmingen), samples were analyzed immediately using an LSR Fortessa (BD Biosciences). Data were analyzed using FlowJo software (Treestar). For transduced cells, events were gated on the GFP^+ compartment as indicated.

Measurement of telomerase activity. Telomerase activity was determined using the TeloTAGGG telomerase ELISA kit from Roche according to the manufacturer's instructions from extracts of 2×10^3 viable $CD27^-CD28^-CD4^+$ T cells. The absolute numbers of $CD27^-CD28$ $CD4^+$ T cells were enumerated by Trypan Blue (Sigma), and proliferation was determined by Ki67 staining as described[39]. Telomerase activity is expressed as proportional to fold increase at 450 nm absorbance emission of triplicate wells ± s.e.m.

Proliferation assays. Four days after transduction, proliferation of activated senescent human $CD27^-CD28^-CD4^+$ T cells was assessed by overnight probing with $[^3H]$thymidine and expressed as fold increase in $[^3H]$thymidine incorporation (cpm) of triplicate wells ± s.e.m. Alternatively, antigen-specific responsiveness of senescent human $CD27^-CD28^-CD4^+$ T cells was assessed by staining for the cell cycle related nuclear antigen Ki67 4 d after activation with autologous VZV-pulsed APCs.

Mice. *Sesn1*$^{-/-}$ mice were generated from *Sesn1*$^{+/-}$ embryonic stem (ES) cells in the C57BL/6 background, obtained from EUCOMM. These cells were created by a targeted gene trap approach and contain reporter-tagged insertion within intron 5 of the *Sesn1* gene with a strong splice acceptor site expressing a β-Gal-Neo fusion protein that disrupts the *Sesn1* ORF. The *Sesn1*$^{+/-}$ mice, produced from ES cells, were backcrossed to wild-type C57BL/6 mice ($n = 5$) to eliminate any nonspecific genetic aberrations that may present in the chromosomes from the ES cells. After the backcrossing, the *Sesn1*$^{+/-}$ mice were interbred to generate *Sesn1*$^{-/-}$ mice, which were found to be fully viable and fertile. *Sesn1*$^{+/-}$ littermates were used as a control strain, and housed with the *Sesn1*$^{-/-}$ mice throughout the course of aging experiments. The absence of sestrin 1 mRNA and protein was confirmed by RT-PCR and immunoblot analyses of splenocytes (**Supplementary Fig. 6**) as well as other tissues (data not shown). Mice were maintained in filter-topped cages and were given free access to autoclaved chow diet and water, according to US National Institutes of Health (NIH) and institutional guidelines. All animal aging studies were overseen by the University Committee on Use and Care of Animals (UCUCA) at the University of Michigan.

Mouse studies. Age-matched (20-month-old) mice were imported from the University of Michigan, rested for 10 d, and then used for *in vivo* studies. Control *Sesn1*$^{+/-}$ and *Sesn1*$^{-/-}$ mice were subcutaneously injected with the seasonal influenza vaccine FLUAD (Novartis; 1:20 of the human dose). A saline solution (PBS) was used as control injection. Five days later, animals were euthanized in a CO_2 chamber, and their spleens collected and processed for splenocyte isolation. Mouse $CD4^+$ T cells were obtained from splenocytes by immunomagnetic separation (Miltenyi Biotec) and immediately analyzed for phenotypic, signaling and functional profiles by either flow cytometry or ImageStream, as indicated. $CD4^+$ phenotypic analysis was performed by surface staining to CD62L and CD44. For recall responses, control *Sesn1*$^{+/-}$ and *Sesn1*$^{-/-}$ $CD4^+$ T cells were rechallenged with control *Sesn1*$^{+/-}$ APCs pre-loaded with FLUAD (1:100, 1:50 and 1:25 of the human dose), then IL-2^+, IFN-γ^+ or Ki67^+ T cells were analyzed 18 h later by flow cytometry. All *in vivo* studies were undertaken at University College London (license no. 70/7354).

Antibody titration. *Sesn1*$^{+/-}$ and *Sesn1*$^{-/-}$ mice were vaccinated with FLUAD as described above. One week later, mice were sacrificed, and blood samples were immediately collected by cardiac bleeding. Levels of circulating immunoglobulins (IgGs) were analyzed using a serum dilution of 1:200 in 0.1% nonfat dry milk 0.5% Tween-20 in PBS, as described[33]. Samples were incubated on Nunc Maxisorp plates precoated with FLUAD overnight (1:40; for 18 h at 4 °C), or PBS as background control. Plates were washed three times with 0.5% Tween-20 in PBS and blocked with 200 µl 4% nonfat dry milk (GE Healthcare). Antigen-specific serum antibodies were detected using horseradish peroxidase (HRP) conjugated antibodies (anti-mouse IgG, Sigma-Aldrich) at 1:3,000 dilution in 0.1% nonfat dry milk 0.5% Tween-20 in PBS, at room temperature. Substrate activity was detected using 100 µL tetramethylbenzidine (TMB) substrate (BD Biosciences) and stopped using 50 µL 2N H_2SO_4 per well. Circulating vaccine-specific IgG levels were determined by ELISA (absorbance emission at 450 nm) of triplicate wells ± s.e.m.

Inhibition of sestrin-MAPK signaling *in vivo*. Aged-matched mice (16 months) were injected intraperitoneally (i.p.) with the Erk inhibitor FR18024 (25 mg/kg), the Jnk inhibitor SP-600125 (16 mg/kg) or the p38 inhibitor SB-203580 (10 mg/kg) individually or together. Drug vehicle was DMSO. Three hours later, mice were vaccinated with FLUAD as above. Triple and individual MAPK inhibition treatments were then repeated daily. Five days later, mice were culled, spleens collected and the impact of *in vivo* blocking MAPK signaling on immune responsiveness was analyzed in sestrin 2^+ T and B cell populations.

Analysis of the sMAC *in vivo*. Primary human or mouse $CD4^+$ T cells were fixed with 2% paraformaldehyde, permeabilized with methanol and stained for sestrin 2, p-Erk, p-Jnk and p-p38 directly *ex vivo,* as above described. For human experiments, $CD4^+$ T cells were separated into early-differentiated and highly differentiated populations according to their relative CD27 and CD28 expression profiles from either young (20–35 years old) or old (70–85 years old) donors. All samples were run on an Amnis ImageStream cytometer using INSPIRE software, magnification 60×. Data were analyzed using IDEAS v.6.1 software (Amnis). Colocalization signals were determined on a single cell basis using bright detail similarity (BDS) score analysis. Colocalization was considered with BDS of ≥2.0.

Gel-filtration chromatography. A Superdex 200 (GE Healthcare) gel filtration column was first equilibrated with 1.5 CV of endotoxin free PBS (Hyclone) at room temperature. Sestrin 2 complexes were injected at time 0 (500 µl) and eluted using a single isocratic wash, fractions collected, and analyzed by ELISA-based binding assays (absorbance at 450 nm) across the spectrum for the indicated proteins. Phosphorylated MAPKs were detected using Phospho-Tracer ELISA kits (Abcam) as above described. For detection of Mios (MBS9330396); RagA (MBS9334409); and RagB (MBS9318748). The column was calibrated with protein markers as described[18].

Statistical analysis. GraphPad Prism was used to perform statistical analysis. For pairwise comparisons, a paired Student's *t*-test was used. For three matched groups, a one-way analysis of variance (ANOVA) for repeated measures with a Bonferroni post-test correction was used. $^*P < 0.05$, $^{**}P < 0.01$ and $^{***}P < 0.001$ throughout. For correlation studies, Pearson correlation test was used.

Data availability. The data generated or analyzed during this study are included in the published article and its supplementary information files.

Uncropped immunoblots are shown in **Supplementary Figures 8** and **9**; individual ImageStream channels are shown in **Supplementary Figure 10**. Data not shown can be obtained from the corresponding authors upon reasonable request.

38. Escors, D. *et al.* Targeting dendritic cell signaling to regulate the response to immunization. *Blood* **111**, 3050–3061 (2008).
39. Plunkett, F.J. *et al.* The loss of telomerase activity in highly differentiated $CD8^{+}CD28^{-}CD27^{-}$ T cells is associated with decreased Akt (Ser473) phosphorylation. *J. Immunol.* **178**, 7710–7719 (2007).

doi:10.1038/ni.3665